

# RSC Advances



This is an *Accepted Manuscript*, which has been through the Royal Society of Chemistry peer review process and has been accepted for publication.

*Accepted Manuscripts* are published online shortly after acceptance, before technical editing, formatting and proof reading. Using this free service, authors can make their results available to the community, in citable form, before we publish the edited article. This *Accepted Manuscript* will be replaced by the edited, formatted and paginated article as soon as this is available.

You can find more information about *Accepted Manuscripts* in the [Information for Authors](#).

Please note that technical editing may introduce minor changes to the text and/or graphics, which may alter content. The journal's standard [Terms & Conditions](#) and the [Ethical guidelines](#) still apply. In no event shall the Royal Society of Chemistry be held responsible for any errors or omissions in this *Accepted Manuscript* or any consequences arising from the use of any information it contains.

1 **Competitive biosorption of Cr(VI) and Zn(II) ions in single-**  
2 **and binary-metal systems onto a biodiesel waste residue using**  
3 **batch and fixed-bed column studies**

4

5 Shanmugaprakash M<sup>1</sup>, Sivakumar V<sup>2\*</sup>

6

7 <sup>1</sup>*Downstream Processing Laboratory, Department of Biotechnology, Kumaraguru*

8 *College of Technology, Coimbatore 641 049, India.*

9 <sup>2</sup>*Department of Chemical Engineering, A.C. Tech, Anna University, Chennai-600 025,*

10 *India.*

11

12

13

14

15

16

17

18

19

20 \*Corresponding author. Tel.: 0422-266 1100; Fax: 0422-266 9406.

21 *E-mail address:* sunbioin@gmail.com

22

23

24

## 25 Abstract

26 A feasible biosorption process for the removal of Cr(VI) and Zn(II)  
27 ions from single and binary solutions onto a defatted *pongamia* oil cake  
28 (DPOC) was investigated. The maximal biosorption capacities of Cr(VI) and  
29 Zn(II) ions in single metal solutions were found to be 166.60 mg/g and  
30 123.45 mg/g, respectively. Due to the internal competition effect, the  
31 biosorption capacity of Cr(VI) and Zn(II) ions in the binary system was  
32 reduced to 125.10 mg/g and 83.30 mg/g, respectively. Experimental data  
33 were well described by Freundlich isotherm. Kinetic studies were also  
34 preformed and the rate kinetics was followed with pseudo-second order  
35 model. Thermodynamic parameters such as Gibbs free energy ( $\Delta G^\circ$ ),  
36 entropy ( $\Delta S^\circ$ ) and enthalpy ( $\Delta H^\circ$ ), were estimated in both single and binary  
37 systems, which showed that biosorption on the DPOC was of exothermic  
38 nature. In the column study, biosorption of metals using single and binary  
39 solutions was fitted well by the Thomas model.

40 **Keywords:** Single and binary metal systems, column study, Cr(VI),  
41 defatted *pongamia* oil cake, equilibrium isotherm, kinetics

42

43

44

45

46

47

## 48 **Introduction**

49 Modern day scientific advancements have led to the release of huge  
50 quantities of aqueous effluents containing highly toxic pollutants such as  
51 heavy metals, dyes and radio-nucleotides into the environment. Also in  
52 recent years, water contamination due to heavy metals has been reported as a  
53 major concern. Chromium and zinc are among the widely employed heavy  
54 metals in several electroplating, leather, tanning, textile, dyeing and metal  
55 finishing industries.<sup>1</sup> In aqueous water, chromium generally exists in two  
56 different oxidative forms (Cr(III) and Cr(VI)).<sup>2</sup> Cr(VI) in particular  
57 possesses human toxicity properties causing skin irritation, lung cancer etc.<sup>3</sup>  
58 Zinc at lower concentrations is an essential element for humans stimulating a  
59 number of biochemical reactions within the cell and it also plays a vital role  
60 in the immune system. However, higher concentrations of both chromium  
61 and zinc in the body elicits toxic effects.<sup>4</sup> According to the U.S.  
62 Environmental protection Agency (EPA), the permissible limits for Cr(VI)  
63 and Zn(II) ions in drinking water should not exceed 0.05 mg/L and 5.0  
64 mg/L.<sup>5</sup>

65 In recent years, many physical and chemical methods like adsorption,  
66 chemical electro coagulation, precipitation, filtration, electro-dialysis,  
67 membrane-based separation etc have been employed for the removal of  
68 heavy metals from effluents.<sup>6</sup> Despite different limitations such as high  
69 separation costs and problems related to residual metal sludge disposal,  
70 some of these techniques have been reported to be effective.<sup>7</sup> Keeping in  
71 mind the contemporary scenario, the need to search for more optimal  
72 technologies involving local resources like plant-based agro-wastes for the

73 removal of metals from effluents has arisen.<sup>8</sup> Biosorption is an active non-  
74 metabolic natural process based upon the capacity of biological materials to  
75 remove metals by employing methods of ion exchange, micro-precipitation,  
76 adsorption and coordination.<sup>9</sup> Economic viability studies indicate that  
77 biosorption has greater advantages over other existing technologies such as  
78 ion exchange or activated carbon adsorption owing to the facts that  
79 biosorbents are economical, easily subjected to chemical surface  
80 modification leading to increased efficiency, exposed to lesser  
81 environmental interferences, capable of recovering precious metals and also  
82 easily adaptive to existing continuous systems.<sup>10</sup> These biosorbents endow  
83 reductive and adsorptive characteristics on the different functional groups  
84 present on the surface. It is evident from existent literature that various agro-  
85 based bio-products have already been employed as low-cost biosorbents as  
86 observed in the cases of fertilizer industrial waste<sup>11</sup>, orange peel waste<sup>12</sup>,  
87 soya bean meal waste<sup>13</sup>, tea factory waste<sup>14</sup>, seaweed<sup>15</sup>, *Jatropha* oil cake<sup>16</sup>  
88 etc.

89 One of the major problems in demonstrating metal ion biosorption from  
90 industrial effluent is that it contains more than one metal ion in aqueous  
91 solution. Hence, it is necessary to focus on sorption of multi-component  
92 system.<sup>17</sup> However, literature pertaining to simultaneous biosorption of  
93 Cr(VI) and Zn(II) using plant-based derivatives in multi-component systems  
94 is quite scarce. Therefore, the objective of the present study undertaken was  
95 to investigate the biosorption of Cr(VI) and Zn(II) ions onto DPOC from  
96 both single and binary metal solutions in batch as well as continuous  
97 systems. Related biosorption isotherms, kinetics and thermodynamics were  
98 studied in detail for a better understanding of metal adsorption

99 characteristics. Finally, the structural and surface functional groups of the  
100 biosorbent (DPOC) were analysed using FTIR and SEM-EDAX.

## 101 **Materials and methods**

### 102 **Preparation of biosorbent and Characterization**

103 *Pongamia* oil cake (POC) used in the study was sourced from local oil mills.  
104 The collected oil cakes were dried under the sun and impurities removed  
105 manually. The dried biosorbent was powdered using a mortar and pestle.  
106 The biosorbent was then sieved to obtain uniform sizes of 250  $\mu\text{m}$  and  
107 further dried at 110  $^{\circ}\text{C}$  for 24 h in an oven. The resultant biosorbent was  
108 then defatted using hexane in a soxhlet extractor (model No: 212, Sigma  
109 Instruments Ltd., Chennai, India) to eliminate the residual oil present in the  
110 oil cakes. The defatted biosorbent (DPOC) stock was stored in air-tight  
111 containers for future experimental purpose.<sup>19</sup> Fourier Transformed Infra red  
112 Spectroscopy (FTIR) analysis was performed using a Shimadzu  
113 spectrophotometer to identify various functional groups present on the  
114 surface of the DPOC preceding and following biosorption under different  
115 experimental conditions (KBr technique). Spectra in the range of 400-4000  
116  $\text{cm}^{-1}$  was recorded. For SEM and Energy dispersive X-ray analysis, samples  
117 were gold/carbon coated and vacuumed (10-15 minutes) for electron  
118 reflection prior to analysis using a JEOL-JSM 6400 scanning electron  
119 microscope.

### 120 **Batch biosorption studies**

121 A stock solution (1000 mg/L) of Cr(VI) and Zn(II) ions was prepared by  
122 dissolving appropriate quantities of potassium dichromate and zinc sulphate  
123 salts in suitable buffers to maintain a constant pH throughout the study. All

124 the chemicals used in this research were of analytical reagent grade and  
125 purchased from Himedia Ltd., India. The speciation distribution of the heavy  
126 metal ions studied was calculated using the MEDUSA computer program  
127 developed by the Royal Institute of Technology (KTH), Sweden.<sup>18</sup> The  
128 experimental procedure and conditions adopted were based on our previous  
129 study.<sup>19</sup> To study the effect of pH, the pH of the solution was adjusted  
130 between 1.0 to 9.0 using 0.1 mol/L NaOH or 0.1 mol/L HCl accompanied by  
131 a pH meter (LI 120 Elico Ltd., Hyderabad, India). The pH experiments were  
132 conducted by maintaining 100 mL metal solutions of variable pH at 298 K  
133 for 120 mins along with 0.6 g of DPOC. Isothermal and kinetic studies were  
134 also performed at 298 K. 0.6 g of DPOC was kept constant in 100 mL  
135 volumes of metal solutions of different concentrations (100-500 mg/L) at  
136 different time intervals (0-240 min) at corresponding pH. Similarly, the  
137 binary metal solution experiments were performed as described above with  
138 the pH value optimized to 3.

### 139 **Column biosorption studies**

140 The fixed-bed studies were performed to assess the effect of flow rate and  
141 bed height on the biosorption of Cr(VI) and Zn(II) ions on the DPOC in both  
142 single and binary metal solutions. Column studies were carried out in a glass  
143 column (45 x 2.0 cm), filled with a known quantity of DPOC. In the column,  
144 0.5-mm stainless steel mesh and 1.0 cm glass beads were kept at the bottom  
145 and the top, to support the biosorbent in the column and also to ensure a  
146 closely packed arrangement. A 2.0-cm high layer of glass beads (1.0 mm in  
147 diameter) was placed at the column base, in order to provide a uniform inlet  
148 flow of the solution into the column. The metal solution was pumped  
149 through a peristaltic pump (model no.4651, Miclins, India) connected at the

150 bottom of the column in an upward direction. The treated metal solution was  
151 collected from the top with the same flow rate as the feed stream and  
152 analysed for the metal concentration. All experiments were performed in  
153 duplicate at 298 K and pH 3.0 under room atmospheric pressure. The  
154 breakthrough curves were obtained by plotting the ratio of  $(C/C_0)$  of metal  
155 concentration  $(C)$  at any time  $t$  to initial metal concentration  $(C_0)$  versus time  
156  $(t)$  at different flow rates.

### 157 Analytical methods

158 The residual Cr(VI) ion present in the supernatant was determined by  
159 DPC (1,5-diphenyl carbazide) method. The residual Cr(VI) ions were then  
160 determined from the standard calibration graph. The total chromium and  
161 Zn(II) ions concentration in the samples were estimated by using atomic  
162 adsorption spectroscopy (SL 159, Elico Ltd, Hyderabad, India).

163 The removal efficiency  $R$  (%) of metal ions was then calculated for  
164 each run as

$$165 \quad R(\%) = \frac{C_o - C_f}{C_o} \times 100 \quad (1)$$

166 where  $C_o$  and  $C_f$  are the initial and the final concentrations of the metal ions  
167 present in the residual solution (in milligram per litre), respectively.<sup>4</sup> The  
168 biosorption capacity  $(q_e)$  of a biosorbent, which is obtained from the mass  
169 balance on the adsorbate in a system with solution volume  $V$ , is often used to  
170 acquire the experimental adsorption isotherms. Under experimental  
171 conditions, the adsorption capacities of the biosorbent for each concentration  
172 of metal ions at equilibrium were calculated as



$$173 \quad q_e(\text{mg} / \text{g}) = \frac{C_o - C_e}{M} \times V \quad (2)$$

174 where  $C_o$  and  $C_e$  are the initial and equilibrium concentrations of metal ions  
175 (in milligram per litre) in the test solution, respectively.  $V$  is the volume of  
176 solution (in litre) and  $M$  is the mass of biosorbent (in grams) used for the  
177 experiment. For column studies, the volume of the effluent,  $V_{\text{ef}}$  (in millilitre)  
178 was calculated using the following equation:

$$179 \quad V_{\text{eff}} = Q * t_{\text{total}} \quad (3)$$

180 where  $t_{\text{total}}$  is total time (in minute) and  $Q$  is the volumetric flow rate of the  
181 metal solution inside the column (in millilitre per minute).

182 The total amount of metal solution that passes through the column ( $M_{\text{total}}$ )  
183 was calculated by

$$184 \quad M_{\text{total}} = \frac{C_o * F * t_e}{1000} \quad (4)$$

185 where  $C_o$  is initial metal concentration (in milligram per millilitre),  $F$  is the  
186 volumetric flow rate (in millilitre per minute) and  $t_e$  is exhaustion time (in  
187 minute).<sup>14</sup>

188 The total removal of metal ions with respect to the flow volume was  
189 calculated as follows

$$190 \quad T_{\text{removal}} = \frac{M_{\text{ad}}}{M_{\text{Total}}} * 100 \quad (5)$$

191 where  $M_{\text{ad}}$  is the concentration of the adsorbed metal ions, (in milligrams  
192 per litre).

## 193 **Results and Discussion**

### 194 **Speciation of metal ions in aqueous system**

195 The speciation of aqueous metal ions significantly influences their  
196 interaction with the surface of the adsorbents.<sup>20</sup> The theoretical distribution  
197 of the predominant chemical ions of Cr(VI) and Zn(II) in aqueous solution  
198 versus pH is represented in Fig.1(a) & (b). It is found that at low pH, Cr(III)  
199 and Zn(II) species are present totally in ionic states while they precipitate as  
200 hydroxides at a high pH. From Fig.1(a), Cr(III) species diagram, it is found  
201 that Cr(III) ions predominately exist at a pH of about 2.0, whereas Cr(OH)<sub>4</sub>  
202 ions begin to form above pH 3.0. Between pH 2.0 and 4.0, the free cation  
203 concentration continuously decreases and insoluble hydroxide precipitates of  
204 Cr(OH)<sup>2+</sup> begin to form. From pH 4.0 to 6.0, the amount of insoluble  
205 hydroxides increases while the concentration of the hydroxide complexes  
206 decreases.<sup>12</sup> The Zn(II) species distribution is represented in Fig.1(b) and  
207 the free cation Zn(II) is the predominant species upto pH 6.0 while the  
208 hydroxides (Zn(OH)<sup>+</sup> begin to form at higher pH values (pH>6.0). Between  
209 pH 6.0 and 8.0, the concentration of hydroxide ions increases while the free  
210 cation decreases. Also at this stage, another hydroxide Zn(OH)<sub>3</sub><sup>+</sup> begins to  
211 form. At pH 8.0, the single hydroxide (Zn(OH)<sup>+</sup>) complex is prevalent  
212 accounting to a concentration of about 75 % and the other hydroxide  
213 (Zn(OH)<sub>2</sub>) complex contributes about 25 %.

#### 214 **pH dependence on Cr(III) and Zn(II) ion removal in single system**

215 One of the prime factors affecting the biosorption of metal ions is pH of the  
216 solution , which influences surface charge of the biosorbent, the degree of  
217 ionization of the species present in the solution, the dissociation of  
218 functional groups on the active sites of biosorbent, and the solution metal  
219 chemistry.<sup>20</sup> In the present work, the influence of pH on Cr(VI) and Zn(II)

220 adsorption was studied by varying the pH of the solution from 2.0–7.0, while  
221 keeping all other parameters constant in single metal solution. In fact,  
222 considering the species distribution diagram (SDD) for Cr(VI), between pH  
223 1 and 5, Cr(VI) occurs in solution as negative species:  $\text{HCrO}_4^-$  and  $\text{Cr}_2\text{O}_7^{2-}$ .  
224 In addition, at pH 2, the pH where the authors found the maximum  
225 adsorption of Cr(VI), the main chemical binding groups of the biomass  
226 surfaces are protonated.<sup>21</sup> As a consequence, the surface of biosorbent will  
227 be surrounded by  $\text{H}^+$  ions which enhance the Cr(VI) interaction with binding  
228 sites of the biosorbent due to electrostatic forces.<sup>22,23</sup> The results obtained by  
229 the authors are in agreement with similar results obtained by other  
230 authors.<sup>23,24</sup> In the single system, the maximum Cr(VI) adsorption was  
231 obtained at an acidic pH of 2.0 which decreases with an increase in pH value  
232 as shown in Fig 2. This is due to the surface charge of the DPOC which was  
233 more protonated under acidic pH and competitive negative metal ion  
234 adsorption takes place between positive surface and free chromate ions.<sup>25</sup> In  
235 aqueous solution, Cr(VI) exists as  $\text{HCrO}_4^-$ ,  $\text{Cr}_2\text{O}_7^{2-}$ , at optimum sorption pH  
236 (pH >2.0). Among those, the predominant form of hexavalent chromium at  
237 acidic pH is  $\text{HCrO}_4^-$ , which arises from the hydrolysis reaction of the  
238 dichromate ion ( $\text{Cr}_2\text{O}_7^{2-}$ ) and the increase in pH shifts the concentration of  
239  $\text{HCrO}_4^-$  to  $\text{Cr}_2\text{O}_7^{2-}$  and other forms such as  $\text{CrO}_4^-$ . Moreover, the optimum pH  
240 of total chromium removal from aqueous solution was also found to be 2.0

241 However, in the case of Zn(II), the adsorption increased sharply with  
242 the increase in pH and attained the maximum at pH 4.0 and then decreased  
243 slowly. At low pH values the surface of the DPOC becomes more positively  
244 charged, reducing the attraction between Zn(II) ions and functional groups  
245 on the adsorbent. In contrast, higher pH results in facilitation of the metal

246 biosorption, since the DPOC is more negatively charged. As the pH is  
247 increased to 4, more functional groups with a negative charge such as  
248 carboxyl or hydroxyl become exposed with a subsequent increase in  
249 attraction sites to positively charged ions (since  $\text{pH}_{\text{ZPC}} = 5.0$ ), and thus  
250 enhances the biosorption capacity.<sup>16,26</sup> The decrease in biosorption at a  
251 higher pH might be attributed to the speciation of other metal species, such  
252 as the occurrence of  $\text{Zn}(\text{OH})_3$  ions as a result of the dissolution of  $\text{Zn}(\text{OH})_2$ .  
253 Similar results were also observed for the binary system. In the binary  
254 system, due to the high degree of competition on active site between the two  
255 metal ions, the biosorption capacities of Cr(VI) and Zn(II) were maximum at  
256 pH 3 and thereby gets decreased in higher pH. Also from Fig.2, it was  
257 observed that Cr(VI) ions is the dominant species in binary mixtures at  
258 lower pH and maximal removal efficiency was attained for Cr(VI) ions  
259 compared to Zn(II) ions. Therefore, all biosorption experiments were  
260 performed at pH 2 and 4 for Cr(VI) and Zn(II) ions, respectively in single  
261 systems and for the binary system, an optimum pH of 3.0 was chosen for  
262 subsequent experiments.

### 263 **Effect of metal ion concentration on single and binary components**

264 Fig.3 illustrates the time profiles of biosorption of Cr(VI) and Zn(II)  
265 ion in single and binary systems where the initial concentration of each  
266 metal ranges from 100-500 mg/L and adsorbent dosage of 6 g/L. The  
267 biosorption of Cr(VI) and Zn(II) ions onto the DPOC is faster in the first 50  
268 min and attains equilibrium in 60 min for both cases. From Fig.3, it is  
269 concluded that the metal biosorption involves 2 phases; (i) a very rapid  
270 initial biosorption, followed by a long period of a much slower uptake.  
271 Similar kinetic behaviors can also be seen in a binary system where the

272 sorption of Cr(VI) predominates that of Zn(II) ions. During the initial stage  
273 of biosorption, a large number of vacant active sites are available for  
274 biosorption of Cr(VI) and Zn(II). Moreover, the active sites almost get  
275 saturated with metal ions during initial stages of biosorption. Furthermore,  
276 the metal ions have to pass through farther and deeper into the pores  
277 exhibiting much resistance.<sup>27</sup> This results in the reduction of biosorption  
278 rate during the late period of biosorption. A similar observation was also  
279 reported by Liu et al., (2009).<sup>20</sup>

### 280 **Effect of biosorption capacity on single and binary systems**

281 An experimental study was carried out to investigate the effect in the  
282 biosorption capacity ( $q_{\max}$ ) for various single and binary systems. In single  
283 metal systems (Fig. 4 (a)), the biosorption capacity of Cr(VI) and Zn(II) ions  
284 was found to vary from (18.63-70.11 mg/g) and (15.93-57.03 mg/g).  
285 However, in the binary system it was found that the individual biosorption  
286 capacity of Cr(VI) and Zn(II) decreases at every concentration range when  
287 compared with the single biosorption system (Fig.4(b)). These results  
288 represent an inhibitory effect of the metal ions among them, thereby  
289 resulting in a lower sorption yield. However, the overall adsorption  
290 capacities of the adsorbent were higher as compared with the single sorption  
291 system. This is due to the saturation of different active sites that are  
292 favourable for different metals ions.<sup>17, 25</sup> In the single sorption system, Cr(VI  
293 and Zn(II) ions could be adsorbed on the surface of the DPOC by internal  
294 competition (competition between ions of the same metals) and they were in  
295 competition with  $H^+$  for adsorption sites.<sup>27</sup> But, in the binary system, there  
296 was an internal competition and competition among themselves for  
297 precipitation and for adsorption sites. In general, three possible types of

298 biosorption behaviours are exhibited: (1) synergism (the effect of the  
299 mixture is greater than that of each of the individual adsorbates in mixture  
300 ( $q_{\min}/q_{\max}>1$ )) (ii) antagonism (the effect of the mixture is less than that of  
301 each of the individual adsorbates in mixture ( $q_{\min}/q_{\max} <1$ )) and (iii) non-  
302 interaction (the mixture has no effect on the adsorption of each of the  
303 adsorbates ( $q_{\min}=q_{\max}$ ). From Table 1, it is observed that the binary system of  
304 Cr(VI)-Zn(II) ions was found to be antagonistic. It has been said that in  
305 general, the greater the atomic weight, electronegativity, electrode potential  
306 and ionic size, the greater will be the affinity for sorption.<sup>28</sup> It is evident  
307 from Table S1 that atomic radii and Vander Waals radii are dominant factors  
308 for the biosorption of Cr(VI) ion onto the DPOC when compared with Zn(II)  
309 ions . The order of biosorption is Cr(VI)>Zn(II) onto the DPOC, was  
310 consistent with the physicochemical properties of metal ions under study.  
311 Thus, the binary biosorption of Cr(VI) ions is more competitive than Zn(II)  
312 ions in solution and those sorbed onto the surface of the DPOC. A similar  
313 observation was found by Anandkumar and Mandal (2012).<sup>25</sup>

#### 314 **Equilibrium modelling of isotherm for single and binary biosorption**

315 To evaluate the designing of biosorption system, the equilibrium data of  
316 Cr(VI) and Zn(II) ion in both single and binary systems were analysed using  
317 Langmuir, Freundlich, Temkin and Halsey isotherms.

318 Langmuir isotherms assume that the adsorbed layer is a homogenous surface  
319 by monolayer sorption and all active sites are equal, resulting in equal  
320 energies and enthalpies of adsorption.<sup>29</sup>

321 The linearised form of Langmuir can be expressed as

$$322 \quad \frac{C_e}{q_e} = \frac{1}{Q_o b} + \frac{C_e}{Q_o} \quad (6)$$

323 where  $C_e$  is the equilibrium concentration of adsorbate (in milligrams per  
324 litre),  $q_e$  is the amount of metal adsorbed per gram at equilibrium (in  
325 milligrams per gram),  $Q_o$  is the maximum monolayer adsorption capacity ((in  
326 milligrams per gram) and  $b$  is a constant relating the rate of the reaction (in  
327 litre per milligram). From Table 1, it is clear that the maximum sorption  
328 capacity for Cr(VI) and Zn(II) was 166.60 and 123.45 (in milligrams per  
329 gram) in the single sorption system and 125.10 and 83.30 (in milligrams per  
330 gram) in the binary sorption system, respectively. The decrease in the  
331 sorption capacity while using the binary system is due to the internal  
332 competition between the Cr(VI) and Zn(II) ions. Similar results have been  
333 reported by other researchers also.<sup>28</sup>

334 The Freundlich isotherm model proposes a multilayer sorption with a  
335 heterogeneous energetic distribution of active sites, accompanied by  
336 interaction between sorbed molecules.<sup>30</sup> The general form of the model is  
337 represented as

$$338 \quad q_e = K_f C_e^{1/n} \quad (7)$$

339 where  $K_f$  stands for Freundlich constant related to adsorption capacity ((in  
340 milligrams per gram) (in litre per milligram))<sup>1/n</sup> and  $n$  stands for  
341 heterogeneous factor related to adsorption intensity. The Freundlich equation  
342 is expressed linearly as

$$343 \quad \ln q_e = \ln K_f + \frac{1}{n} \ln C_e \quad (8)$$

344 The values of  $K_f$  and  $n$  were obtained from the linear plot of  $\ln q_e$  and  $\ln C_e$ .

345 For Cr(VI) and Zn ions, the Freundlich values ( $n$ ) are 1.38 and 1.17 in  
346 single and binary systems. According to Table 1, the adsorption of an  
347 adsorbate is favourable when  $n > 1.0$ . Our results clearly indicate that the  
348 DPOC can be effectively employed for the removal of Cr(VI) and Zn(II)  
349 ions from aqueous solution. Based on the  $K_f$  values, metal binding affinity  
350 of the DPOC was in the order of Cr(VI) > Zn(II) ion.

351 The Temkin isotherm model contains a factor that specifically takes into  
352 account only the adsorbent-adsorbate interactions by neglecting the  
353 extremely low and high values of concentration and it is assumed that, the  
354 fall in the heat of sorption is more linear than logarithmic, as implied in the  
355 Freundlich equation.<sup>31</sup>

356 The linearised form of Temkin equation is expressed by the following  
357 equation:

358

$$359 \quad q_e = \frac{RT}{b_T} \ln A_T + \frac{RT}{b_T} \ln C_e \quad (9)$$

360 where  $R$  is the universal gas constant (8.314 J/mol/K),  $T$  is the absolute  
361 temperature (in Kelvin),  $b_T$  represents Temkin isotherm constants (in Joule  
362 per mol),  $A_T$  represents Temkin isotherm equilibrium binding constant (in  
363 litre per gram).  $A_T$  and  $b_T$  were determined from the slope and intercepts of  
364 the plots obtained by plotting  $q_e$  versus  $\ln C_e$  and the calculated parameters at  
365 303K are listed in Table 1 for single and binary systems. Higher  $R^2$  values  
366 indicate the interaction between metals ions and DPOC.



367 The Halsey isotherm<sup>32</sup> is usually used for multilayer adsorption systems and  
368 it is linearly expressed as

$$369 \quad \ln q_e = \left[ \frac{1}{n} \ln k_h \right] - \frac{1}{n} \ln \left( \frac{1}{C_e} \right) \quad (10)$$

370 where  $k_h$  and  $1/n$  are the Halsey constant and exponent, respectively. The  
371 values of  $k_h$  and  $1/n$  were obtained by plotting  $\ln q_e$  and  $\ln \left( \frac{1}{C_e} \right)$  and the  
372 values are given in Table 1. The good linear fitting by higher correlation  
373 coefficients indicates the heteroporosity of DPOC.<sup>26</sup> Based on the linear  
374 regression coefficient value ( $R^2$ ), the equilibrium data could well be  
375 interpreted by the Freundlich isotherms followed by Langmuir, Temkin and  
376 Halsey isotherms.

### 377 **Biosorption kinetics**

378 Kinetics is of paramount importance in determining the rate of adsorption  
379 and also in describing the solute uptake rate which reflects the resistance  
380 time of the adsorption process. In the present study, two kinetic models  
381 namely, the pseudo first-order and pseudo second-order models at different  
382 metal ion concentrations have been tested in order to predict the adsorption  
383 data of Cr(VI) and Zn(II) ions onto the DPOC as a function of time.  
384 Adsorption kinetics is expressed as the amount of metal adsorbed on the  
385 surface at equilibrium  $q_e$  (in milligram per gram) and the fitness of the model  
386 is accredited by  $R^2$  value.

387 The pseudo first-order model assumes that a metal ion gets adsorbed on one  
388 active site of the sorbent surface and is represented by the following scheme:



390 where  $A_d$  is the active site present on the surface of the sorbent and it  
 391 was proposed by Lagergren<sup>33</sup> and is expressed as follows:

$$392 \quad \ln(q_e - q_t) = \ln q_e - k_1 t \quad (12)$$

394 where  $k_1$  is the rate constant (1/minutes),  $q_e$  and  $q_t$  are the amounts of metal  
 395 ions adsorbed on the surface at equilibrium (in milligrams per gram) and at  
 396 any time  $t$  (in minutes).

397 A plot of  $\ln(q_e - q_t)$  versus time was drawn, and the values of  $k_1$  and the  
 398 calculated  $q_e$  was determined from the slope and intercept respectively and  
 399 values are given in Table 2.

400 Similarly, the pseudo second-order model assumes that one metal ion is  
 401 adsorbed onto two active sites, as represented by the following equation



403 Mathematical expression of second-order equation is given as follows<sup>34</sup>:

$$404 \quad \frac{t}{q_t} = \frac{1}{q_e^2 k_2} + \frac{t}{q_e} \quad (14)$$

405 where,  $k_2$  (in gram per milligram per minute) is the pseudo second-order  
 406 rate constant which was determined from the plot between  $t/q_t$  against time.

407 The pseudo first-order constant ( $k_1$ ), pseudo second-order rate  
 408 constants ( $k_2$ ), the calculated  $q_e$  values and the corresponding linear  
 409 regression correlation coefficient values are listed in Tables 2 and 3, for both

410 Cr(VI) and Zn(II) ions, respectively. The value of  $R^2$  for the pseudo first-  
411 order kinetics for both Cr(VI) and Zn(II) ions indicates that this model had  
412 failed to predict the value of  $q_e$ . Meanwhile, the second-order kinetics could  
413 describe the adsorption of Cr(VI) and Zn(II) ions with high correlation  
414 coefficient ( $R^2$ ) highlighting that the rate-controlling mechanism is the  
415 chemical adsorption process, which is a complex in nature. Similar  
416 observation was observed by other researchers also.<sup>2, 25, 26</sup>

### 417 **Thermodynamic parameters of biosorption of Cr(VI) and Zn(II) in** 418 **single and binary systems**

419 Thermodynamic parameters explain the feasibility and spontaneous nature  
420 of the biosorption process. The thermodynamic parameter such as  $K$  value  
421 obtained from the Langmuir isotherm model was used to evaluate the  
422 standard Gibbs Free energy ( $\Delta G^\circ$ ) parameters of each single and binary  
423 system for Cr(VI) and Zn(II) ions respectively. As depicted in Table 4, the  
424 changes in the negative values of  $\Delta G^\circ$  at all temperatures confirm the  
425 feasibility of the biosorption process and high affinity of single and binary  
426 adsorption onto the DPOC [293 to 323 K]. As the temperature increased, the  
427 values of Gibbs free energy decreased suggesting that better adsorption  
428 occurs at higher temperatures. This could be attributed to the interaction  
429 between the metal ions on the solid surface, the non-equal competition  
430 which attributes to the heterogeneity of adsorbent surface and the system  
431 gained energy from an external source at high temperatures.<sup>35</sup> The enthalpy  
432 changes of the biosorption of Cr(VI) and Zn(II) ions ( $\Delta H^\circ$ ) in single and  
433 binary systems onto the DPOC were found to be -16.747, 24.89, -34.22 and  
434 -39.63 (in kilo Joule per mole ). As depicted in Table 4, the negative value

435 of  $\Delta H^\circ$  suggests that the process is exothermic in nature and adsorption is  
436 possible through strong binding between single and binary systems of  
437 Cr(VI) ions and sorbent whereas positive  $\Delta H^\circ$  values indicates that the single  
438 and binary Zn(II) ions by the DPOC are endothermic. The positive values of  
439  $\Delta S^\circ$  reflects the increased randomness at the adsorbate-adsorbent interface  
440 during the biosorption of Zn(II) ions in both single and binary systems.<sup>36</sup>  
441 The order of biosorption heat of these heavy metal ions is as follows : binary  
442 Cr(VI)>single Cr(VI) and binary Zn(II)> single Zn(II) system. The  
443 biosorption of Cr(VI) with high enthalpy changes represents that the systems  
444 are very temperature-sensitive whereas the biosorption of Zn(II) in the  
445 binary system having low-enthalpy changes suggests that the systems are  
446 relatively temperature insensitive in nature.<sup>37</sup>

#### 447 **Fixed-Bed Column Studies**

448 The breakthrough curves are very important characteristics for determining  
449 and evaluating the sorbents for continuous treatment of the metal-laden  
450 effluents on an industrial scale operation. The breakthrough time ( $t_b$ ) shows  
451 the time at which the outlet metal concentration reached the initial  
452 concentration, and the exhaustion time ( $t_e$ ) represents the time at which the  
453 outlet heavy metal concentration exceeded 95% of the inlet metal  
454 concentration. The breakthrough curves were obtained for the biosorption of  
455 Cr(VI) and Zn(II) ions onto the DPOC from single and binary solutions by  
456 varying the flow rate [(10, 15, and 20)] (in millilitre per minute) using a  
457 constant bed height (5 cm) and having inlet metal concentration of 100  
458 mg/L. From Table 5, it is clear that as the flow rate is increased, the metal  
459 adsorption capacity, the breakthrough and exhaustion time were reduced, for  
460 both single and binary systems. This may be due to the unavailability of a

461 sufficient retention time for the heavy metal molecule within the bed at  
462 higher flow rates and the limited diffusivity of the solute into the sorptive  
463 sites or pores of the biomass.<sup>38,39</sup> Slower flow rate is favoured, if  
464 intraparticle mass transfer controls the process and higher flow rate is  
465 favoured, if external mass transfer controls the process.<sup>35</sup>

466 The Thomas model<sup>40</sup> is one of the widely applied models for continuous  
467 flow systems, which can be represented as

$$468 \ln\left(\frac{C_o}{C_t} - 1\right) = \frac{K_{TH}q_o w}{Q} - K_{TH}C_o t \quad (15)$$

469 The Thomas model constants  $K_{Th}$  and  $q_o$  were determined by plotting

470  $\ln\left(\frac{C_o}{C_t} - 1\right)$  versus time  $t$ , at a given flow rate. The Thomas model assumes

471 Langmuir kinetics of adsorption-desorption, plug flow behaviour and  
472 second-order reversible reaction kinetics. The above model is suitable for  
473 adsorption processes where external and internal diffusion limitations are  
474 absent. From Table 5, it is observed that as the flow rate increases, the value  
475 of  $K_{Th}$  was also increased which represents that the mass transfer resistance  
476 present on the surface of the DPOC could be decreased. The Thomas model  
477 gave good fit for the given experimental and theoretical data, at the flow rate  
478 examined and as presented in Fig. 5.

#### 479 **FT-IR and SEM-EDX analyses of biosorbent**

480 FTIR analysis was used to describe the nature of the bonds present and  
481 allows the identification of different functional groups present on the surface  
482 of the DPOC. The FTIR spectra were plotted with wavenumber ranging  
483 from 400-4500  $\text{cm}^{-1}$  in the x-axis and % transmittance on the y-axis (Fig.  
484 S1). The DPOC showed the typical bands attributing to cellulose,

485 hemicellulose and lignin, which was indicative of the ligneous nature of  
486 DPOC. The prominent bands in the pristine DPOC were at 3425.56  $\text{cm}^{-1}$  (O-  
487 H stretching vibration of cellulose), 2924.09  $\text{cm}^{-1}$  (C-H stretching in lignin),  
488 2854.65  $\text{cm}^{-1}$  (C-H stretching in lignin), 2376.30  $\text{cm}^{-1}$  (C-O stretch in  
489 primary alcohols), 1658.78  $\text{cm}^{-1}$  (C-H stretch), 1442.75  $\text{cm}^{-1}$  (O-H in plane  
490 bending), 1242.16  $\text{cm}^{-1}$  (aromatic ring vibration), 1157.29  $\text{cm}^{-1}$  (C-O-C  
491 asymmetrical stretching), 1026.13  $\text{cm}^{-1}$  (C-O, C=C, and C-C-O stretching),  
492 and 879.54  $\text{cm}^{-1}$  (glycosidic linkage in hemicellulose).<sup>11</sup> After biosorption  
493 of Cr(VI) and Zn(II) from both single and binary systems, there is a change  
494 in band intensity and frequency of the IR signals of some functional groups  
495 onto the DPOC. Shifts in the band position of 3425.58  $\text{cm}^{-1}$ , 2376.30  $\text{cm}^{-1}$ ,  
496 1242.16  $\text{cm}^{-1}$ , 1157.29  $\text{cm}^{-1}$  and 879.54  $\text{cm}^{-1}$  to 3410.15  $\text{cm}^{-1}$ , 2384.02  $\text{cm}^{-1}$   
497 <sup>1</sup>, 1249.21  $\text{cm}^{-1}$ , 1149.57  $\text{cm}^{-1}$ , 1018.41  $\text{cm}^{-1}$  and 864.11  $\text{cm}^{-1}$ , respectively  
498 were indicative of Cr(VI) and Zn(II) ions binding to these functional groups  
499 during biosorption process.<sup>16</sup> This may be due to the interaction between  
500 ionized functional groups present on the surface of the DPOC with protons  
501 or metal ions present in the aqueous solutions.<sup>25</sup> Notably, the shift in  
502 3425.58  $\text{cm}^{-1}$  in Cr(VI)-Zn(II) adsorbed on the DPOC indicates the O-H  
503 group involvement in the metal binding through electrostatic interaction.

504 The SEM and EDAX micrographs of the pristine DPOC system, are as  
505 shown in Fig S2 (a) and (b), respectively. The raw DPOC has a number of  
506 pores on the surface of DPOC which get decreased after treating with metal  
507 solution. This may be due to the significant possibility of the chromium and  
508 zinc ions adsorbed onto the pores and the remaining trapped(Fig. S2(c)).  
509 Energy dispersive x-ray (EDAX) analysis was carried out to evaluate the  
510 adsorption of Cr(VI) and Zn(II) ions onto the DPOC. EDAX spectrum for

511 the pristine DPOC represents the presence of Cl, K, S and O in the structure  
512 but did not have any characteristic signal of Cr(VI) and Zn(II) ions on the  
513 surface of the raw DPOC (Fig.S2 (b)). An EDAX spectrum was also  
514 recorded for the Cr(VI) and Zn(II) ions-adsorbed DPOC after treating with  
515 binary mixtures (100 mg/L of Cr(VI) and 100 mg/l of Zn(II) ) solution  
516 (Fig.S2 (d)). The EDAX spectrum gives characteritics peaks for both Cr(VI)  
517 and Zn(II) ions at 5.5 and 6.0 and 1.0 and 8.5, respectively, which confirms  
518 the binding of the Cr(VI) and Zn(II) ions to the surface of the DPOC.

## 519 **Conclusions**

520 In conclusion, we have utilised the DPOC as biosorbent to remove the  
521 Cr(VI) and Zn(II) ions from single and binary solutions in batch and  
522 continues mode. In batch system, the biosorption efficiency was greatly  
523 influenced by pH, dosage, time and temperature. The biosorption behaviour  
524 onto the DPOC was fitted well with the Freundlich isotherm and pseudo  
525 second-order kinetics models. Column experiments showed that the  
526 breakthrough time and exhaustion time decreased with an increasing flow  
527 rate. To the best of our knowledge, there have not been any reports  
528 concerning with biosorption of Cr(VI) and Zn(II) ions from binary system.

## 529 **Acknowledgements**

530 One of the authors (Shanmugaprakash M) is thankful to the management of  
531 Kumaraguru College of Technology, Coimbatore, Tamilnadu, India for  
532 having provided research facilities.

## 533 **References**

- 534 1. S.A. Katz, H. Salem, *VCH Publishers.*, 1994.

- 535 2. M. Shanmugaparakash, S. Venkatachalam, J. PrasanaManikandaKartick, R. Nandush  
536 a, *Environ. Sci. Pollut.*, 2014, **1**, 593-608.
- 537 3. H.J. Gibb, P.S.J. Lees, P.F. Pinsky, B.C. Rooney, *Am. J. Ind. Med.*, 2011, **38**, 115-  
538 126.
- 539 4. U.K. Garg, M.P. Kaur, V.K. Garg, D. Sud, *J. Hazard. Mater.*, 2007, **140**, 60-68.
- 540 5. EPA, 1990., Cincinnati, US.
- 541 6. J. Febrianto, A.N. Kosasih, J. Sunarso, Y.H. Ju, N. Indraswati, S. Ismadji, *J.*  
542 *Hazard. Mater.*, 2009, **162**, 616-645.
- 543 7. N.R. Bishnoi, M. Bajaj, N. Sharma, A. Gupta, *Bioresour. Technol.*, 2004, **91**,  
544 305-307.
- 545 8. V.M. Nurchi, I. Villaescusa, *Coordination Chemistry Reviews.*, 2008, **252**, 1178-  
546 1188.
- 547 9. A.B. Albadarin, C. Mangwandi, G.M. Walker, S.J. Allen, M.N.M. Ahmad, M.  
548 Khraisheh, *J. Environ. Manage.*, 2013, **114**, 190-201.
- 549 10. B. Volesky, *Sorption and biosorption*. BV Sorbex., 2003
- 550 11. V.K. Gupta, A. Rastogi, A. Nayak, *J. Colloid Int. Sci.*, 2010, **342**, 135-141.
- 551 12. V. Lugo-Lugo, C. Barrera-Diaz, F. Urena-Nunez, B. Bilyeu, I. Linares-  
552 Hernandez, *J. Environ. Manage.*, 2012, **112**, 120-127.
- 553 13. A. Witek-Krowiak, D. Harikishore Kumar Reddy, *Bioresour. Technol.*,  
554 2013, **127**, 350-357.
- 555 14. E. Malkoc, Y. Nuhoglu, *J. Hazard. Mater.*, 2006, **135**, 328-336.
- 556 15. V. Murphy, H. Hughes, P. McLoughlin, *Chemosphere.*, 2008, **70**, 1128-1134.
- 557 16. S. Muthusamy, S. Venkatachalam, P.M.K. Jeevamani, N. Rajarathinam,  
558 *Environ. Sci. Pol. R.*, **21**, 593-608.
- 559 17. C. Mahamadi, T. Nharingo, *Bioresour. Technol.*, **101**, 859-864.
- 560 18. W.D. Schecher, D.C. McAvoy, *Environmental Research Software.*, 2001.
- 561 19. M. Shanmugaparakash, V. Sivakumar, *Bioresour. Technol.*, 2013, **148**, 550-559.
- 562 20. C.C. Liu, M.K. Wang, C.S. Chiou, Y.S. Li, C.Y. Yang, Y.A. Lin, *J. Hazard.*  
563 *Mater.*, 2009, **171**, 386-392.
- 564 21. A.E. Martell, & R.M. Smith, *US Department of Commerce, National Institute of*



- 565            *Standards and Technology.*, 2004.
- 566            22. K. Parvathi, & R. Nagendran, *Separation Science and Technology.*, 2007, **42**,
- 567            625-638.
- 568            23. A. Özer, & D. Özer, *J. Hazard. Mater.*, 2003, **100**, 219-229.
- 569            24. M.D. Machado , H.M.V.M. Soares & E.V. Soares , *Water Air and Soil Pollution.*,
- 570            2010, **212**, 199-204.
- 571            25. J.Anandkumar, B. Mandal, *J. Chem. Eng.*, 2012, **7**, 928-939.
- 572            26. B.Kiran, A. Kaushik, *Chem. Eng. J.*, 2008,**144**, 391-399.
- 573            27. Sun, X.-F., Wang, S.-G., Liu, X.-W., Gong, W.-X., Bao, N., Gao, B.-Y, *Colloid.*
- 574            *Int. Sci.*, 2008, **324**, 1-8.
- 575            28. A.S.YesimBurak and T. Kutsal, *Separ. Sci. Technol.*, 2002, **37**, 279-309.
- 576            29. I.Langmuir, *J. Am. Chem. Soc.*, 1918, **40**, 1361-1403.
- 577            30. H.M.F. Freundlich, *J. Phys. Chem.*, 1906, **57**, 1100-1107.
- 578            31. M.I. Temkin, V. Pyzhev, *URSS*,1940, **12**, 217-222.
- 579            32. G. Halsey, *Chem. Phys.*, 2004,**16**, 931-937.
- 580            33. S.Lagergren, *Kungliga Svenska Vetenskapsakademiens Handlingar.*, 1898, **24**,
- 581            1-39.
- 582            34. Y.S. Ho, G.McKay, *Process Saf. Environ. Prot.*, 1998, **76**, 183-191.
- 583            35. N. Atar, A. Olgun, S. Wang, S. Li, *J. Chem. Eng. Data.*, 2011, **56**, 508-516.
- 584            36. Z.M. Aksu and F. Gonen, *Sep. Purific. Technol.*, 2006, **49**, 205-216.
- 585            37. G.L. Uslu, M. Tanyol, *J. Hazard. Mater.*, 2006, **135**, 87-93.
- 586            38. S. Qaiser, A.R. Saleemi, M. Umar, *J. Hazard. Mater.*, 2009, **166**, 998-1005.
- 587            39. M. Shanmugaprakash, V.Sivakumar, M. Manimaran, J. Aravind, *Environ. Prog.*
- 588            *Sustain. Energy.*, 2014, **33(2)**, 342-352.
- 589            40. H.C. Thomas, *Chem. Soc.*,1944, **66**, 1664-1666.

590

591

592

593

594

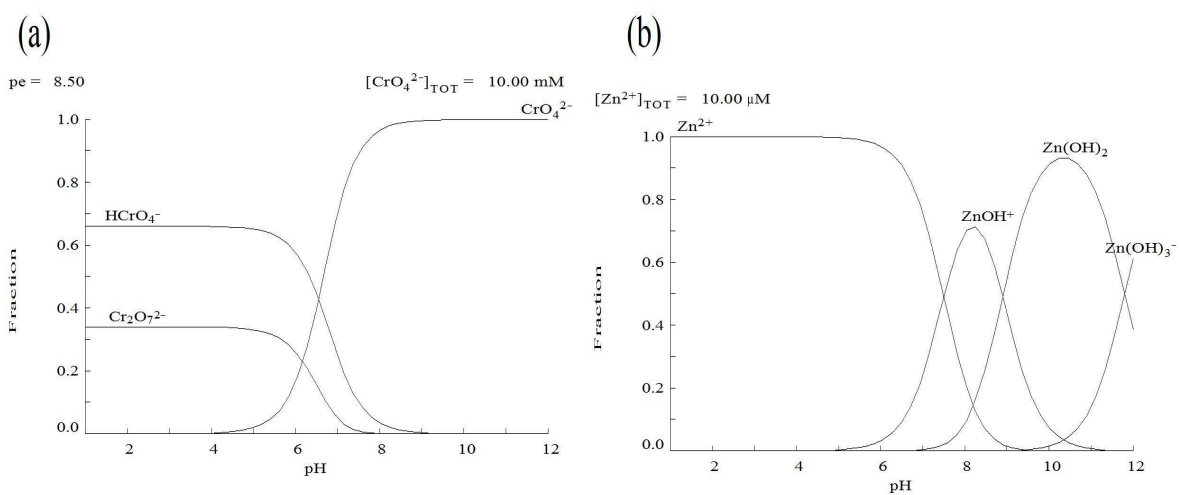
595 **Caption**

- Figure 1 Species distribution diagrams versus pH for (a) 10 mM Potassium di chromate (b) 10 mM Zinc sulphate
- Figure 2 Effect of pH on the biosorption of Cr(VI) and Zn(II) ions from single and binary solutions [initial metal concentration  $C_o = 100$  mg/L (single system),  $C_o = (100$  mg Cr(VI) +100 mg Zn(II))/L (binary system) T: 298 K, Biosorbent dosage: 6 g/ L, contact time: 300 min, agitation speed: 120 rpm]
- Figure 3 Effect of contact time on the biosorption of Cr(VI) and Zn(II) ions from single and binary solutions [pH: 2.0 for Cr(VI) (single), 4.5 for Zn(II) (single) and 3.0 (binary), initial metal concentration  $C_o = 100$  mg/L (single system),  $C_o = (100$  mg Cr(VI) +100 mg Zn(II))/L (binary system), T: 298 K, Biosorbent dosage: 6 g/ L, contact time: 300 min; agitation speed: 120 rpm]
- Figure 4 Competitive biosorption of single and binary metal ions onto DPOC [reaction temperature: 298 K, pH: 2.0 for Cr(VI) (single), 4.5 for Zn(II) (single) and 3.0 (binary), biosorbent dosage: 6 g/ L; reaction time: 240 min (Cr(VI) and 180 min (Zn(II))]
- Figure 5 Breakthrough curves for the Biosorption of Cr(VI) and Zn(II) ions from single and binary solutions [flow rate = 1 mL/min, inlet metal concentration  $C_o = 100$  mg/L(single system),  $C_o = (100$  mg Cr(VI) +100 mg Zn(II))/L (binary system), bed height = 10 cm, pH = 3.0, biosorbent dosage= 13.45 g]

Table 1	Biosorption isotherm parameters of metal biosorption in the single and binary system
Table 2	First-order kinetic constants of Cr(VI) and Zn(II) biosorption in single and binary system onto DPOC
Table 3	Second-order kinetic constants of Cr(VI) and Zn(II) biosorption in single and binary system onto DPOC
Table 4	Thermodynamic parameters of the Cr(VI) and Zn(II) ion biosorption in the single and binary system
Table 5	Column Parameters for the Single and binary metal biosorption onto DPOC at 30 °C

Figure 1

596



597

598

599

600

601

602

603

604

605

606

607

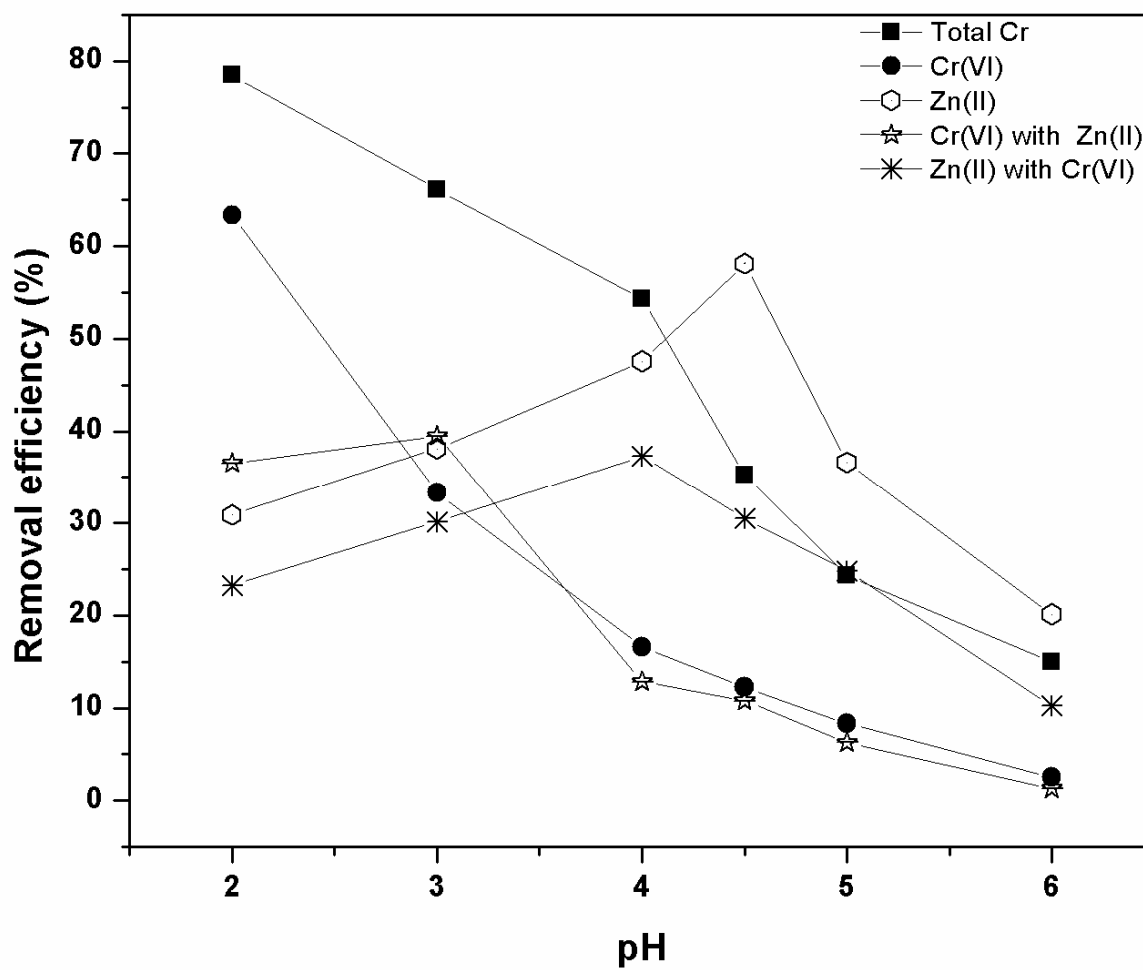
608

609 Figure 2

610

611

612



613

614

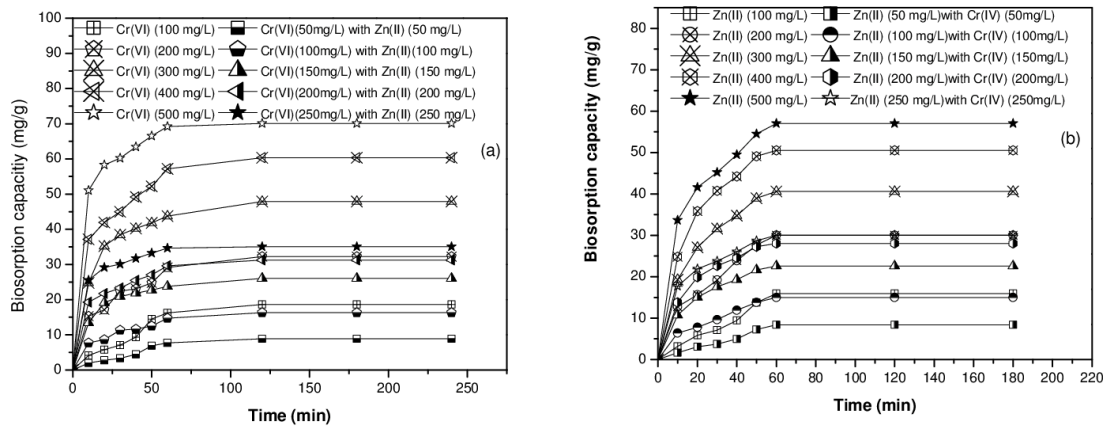
615

616

617 **Figure 3**

618

619



620

621

622

623

624

625

626

627

628

629

630

631

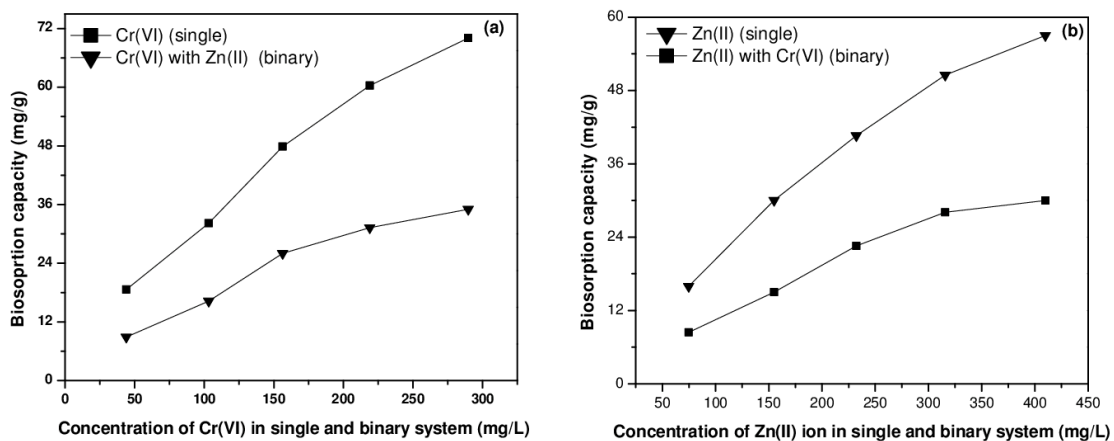
632

633 **Figure 4**

634

635

636



637

638

639

640

641

642

643

644

645

646

647

648

649

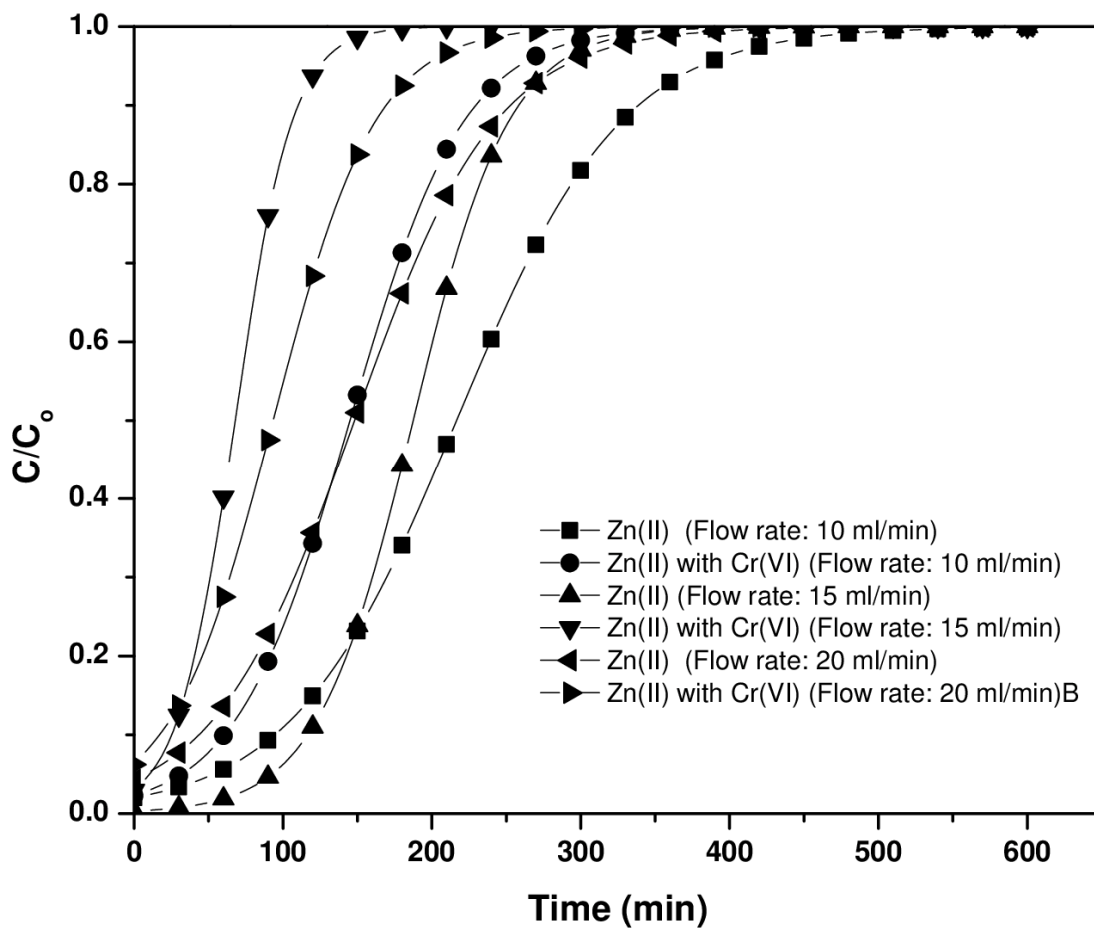
650

651 Figure 5

652

653

654



655

656

657

658



659

660

661

662 Table 1

663 Biosorption isotherm parameters of metal biosorption in the single and binary system

Metal solution in single and binary system	Langmuir		Freundlich				Temkin		Halsey				
	$Q_o$ (mg / g)	$b$ (L/mg)	$Q_{min}/Q_{max}$	$R^2$	$K_F$ ((mg/g) (L/mg) <sup>1/n</sup> )	$n$ (L/mg)	$R^2$	$B_T$ (J/mol)	$A_T$ (L/mg)	$R^2$	$n$	$K_H$	$R^2$
Cr(VI) ( $Q_{max}$ )*	166.6	$2.65 \times 10^{-3}$	1.00	0.93	1.07	1.38	0.99	90.84	0.0387	0.96	1.38	1.25	0.99
Cr(VI)(with Zn(II) ( $Q_{min}$ ))	125.10	$1.06 \times 10^{-3}$	0.75	0.78	0.24	1.17	0.98	155.69	1.48	0.98	0.85	5.45	0.98
Zn(II)( $Q_{max}$ )	123.45	0.0122	1.00	0.88	5.8	1.96	0.97	22.54	5.9	0.88	1.96	31.52	0.97
Zn(II)(with Cr(IV) ( $Q_{min}$ ))	83.30	$1.5 \times 10^{-3}$	0.67	0.90	0.29	1.27	0.99	187.57	0.764	0.98	0.79	4.82	0.99

664 \*References 39

665

666

667

668

669

670

671

672 Table 2

673 First-order kinetic constants of Cr(VI) and Zn(II) biosorption in single and binary system onto  
674 DPOC

675

Metal solution	System	Initial metal ion Concentration (in milligram per liter))	Q <sub>e</sub> (exp) (in mg/g)	Q <sub>e</sub> (cal) (in mg/g)	K <sub>1,ad</sub> (1/ minute)	R <sup>2</sup>
Cr(VI)	Single	100	47.86	46.85	0.0299	0.87
Cr(VI)+Zn(II)	Binary	100	26.06	26.66	0.0251	0.88
Zn(II)	Single	100	40.63	40.12	0.0483	0.84
Zn(II)+Cr(VI)	Binary	100	22.57	23.27	0.0345	0.85

676

677

678

679

680

681

682

683

684

685

686

687

688

689

690

691

692

693

694

695

696 Table 3

697 Second-order kinetic constants of Cr(VI) and Zn(II) biosorption in single and binary system onto  
 698 DPOC

Metal solution	System	Initial metal ion concentration (in milligram per litre))	Q <sub>e</sub> (exp) (in mg/g)	Q <sub>e</sub> (cal) (in mg/g)	K <sub>2,ad</sub> (g/mg/min)	R <sup>2</sup>
Cr(VI)	Single	100	37.03	32.22	1.42x10 <sup>-3</sup>	0.99
Cr(VI)+Zn(II)	Binary	100	18.18	16.27	2.99x10 <sup>-3</sup>	0.99
Zn(II)	Single	100	30.025	21.27	1.036x10 <sup>-3</sup>	0.99
Zn(II)+Cr(VI)	Binary	100	16.94	15.012	3.66x10 <sup>-3</sup>	0.99

699

700

701

702

703

704

705

706

707

708

709

710

711

712

713

714 Table 4

715 Thermodynamic parameters of the Cr(VI) and Zn(II) ion biosorption in the single and binary  
716 system

717

Metal solution	$\Delta H^\circ$ (kJ/mol)	$\Delta S^\circ$ (J/mol/K)	$-\Delta G^\circ$ (J/mol)		
			303 K	313 K	323 K
Cr(VI) single system	-16.744	-45.178	2986.04	2763.32	2072.48
Cr(VI) (with Zn(II) ion)	-34.22	-108.58	1349.38	181.19	18.89
Zn(II) single system	24.89	78.75	1007.03	299.1	570.91
Zn(II) (with Cr(VI) ion)	39.63	120.63	3298.02	1373.12	915.55

718

719

720

721

722

723

724

725

726

727

728

729

730 Table 5

731

732 Column Parameters for the Single and binary metal biosorption onto DPOC at 30 °C

733

Metal solution	Flow rate (ml/min)	Uptake rate (mg/g)	$t_b$ (min)	$t_e$ (min)	Thomas model constants		
					$K_{TH} \times 10^{-5}$ (L/mg/min)	$q_0$ (mg/g)	$R^2$
Cr(VI) single system	10	43.55	120	600	1.0	43.64	0.992
	15	40.42	90	450	2.0	40.53	0.991
	20	37.52	60	300	2.4	37.74	0.994
Cr(VI) (with Zn(II) ion)	10	30.14	100	510	1.1	30.75	0.972
	15	28.88	75	360	2.3	28.92	0.981
	20	28.14	40	270	2.3	28.16	0.995
Zn(II) single system	10	45.21	60	390	1.8	45.33	0.978
	15	43.16	50	300	2.2	43.09	0.975
	20	33.28	45	120	3.1	33.08	0.973
Zn(II) (with Cr(VI) ion)	10	34.25	45	280	2.6	34.12	0.982
	15	28.65	30	270	2.9	28.12	0.992
	20	22.58	30	240	3.5	22.30	0.975

734